Scanning tunneling microscopy of the surface morphology of $YBa_2Cu_3O_x$ thin films between 300 and 76 K

John Moreland, Paul Rice, S. E. Russek, B. Jeanneret, A. Roshko, R. H. Ono, and D. A. Rudman
Electromagnetic Technology Division, National Institute of Standards and Technology, Boulder, Colorado 80303

(Received 29 July 1991; accepted for publication 30 September 1991)

Scanning tunneling microscopy (STM) images of $YBa_2Cu_3O_x$ (YBCO) thin films show different growth mechanisms depending on the deposition method and substrate material. We present images of YBCO films sputter deposited onto MgO and $SrTiO_3$, and laser ablated onto $LaAlO_3$ showing screw dislocation and ledge growth mechanisms. At room temperature we observed an anomalous tunneling conductance near the edge of growth steps which causes a large apparent step-edge height in the STM image. This effect decreases with decreasing temperature, so that the step height approaches the expected value for one unit cell of 1.2 nm at 76 K. This phenomenon reflects changes in either the surface tunneling barrier or tunneling density of states upon cooling.

Scanning tunneling microscopy (STM) has been used extensively to study the atomic structure and growth of high-temperature superconducting (HTS) single crystals. STM images of atomic layers as well as growth steps on the surface of HTS single crystals have been useful for determining their growth mechanisms.[1]

Until recently most of the STM work has been focused on atomic imaging of single crystals since clean, flat surfaces suitable for STM can be prepared. However, Hawley *et al.*[2] and Gerber *et al.*[3] have shown that the STM can be used to image HTS films that have not been prepared in any special way. This was surprising in light of past difficulties encountered when attempting STM on HTS films due to the presence of an insulating surface layer. With improvements in thin-film processing such as *in situ* film growth, the surface quality of films has improved enough to be suitable for STM. In addition, improvements in STM instrumentation have greatly expanded the scanning ranges both laterally (100 μm) and vertically (5 μm). These long scanning ranges combined with the picometer vertical resolution of STM open up a new realm of surface morphology studies with roughness aspect ratios (rise over run) of $<10^{-6}$.

In this letter we present STM images of $YBa_2Cu_3O_x$ (YBCO) thin films that have been either sputtered or laser ablated onto different substrates. The films tested are high-quality *c*-axis oriented superconductors, yet they show strikingly different STM morphologies. The STM images show the growth morphology with adequate resolution for imaging unit cell growth steps on the surfaces of the grains. We find that at room temperature there is an anomalously large tunneling conductance near the edge of the growth steps which manifests itself as a large apparent height variation in the STM image. This effect decreases with decreasing temperature so that the STM step height approaches the expected value for one unit cell of 1.2 nm.

The details of the variable temperature STM apparatus are discussed in other papers.[4,5] The STM head, thermometers, and heater are located in a thermally insulated, dry nitrogen vapor pocket trapped in a liquid nitrogen bath. STM images consisted of 400 line scans per frame with 400 samples per line scan. The images were taken with a PtIr tip at a scan rate of 1.0 lines/s. The tunneling current and voltage were 0.5 nA and 700 mV.

The films for this letter are predominantly *c*-axis oriented. The films were not cleaned or modified in any way before STM imaging. The sputtered films were prepared by off-axis reactive dc magnetron sputtering using an *in situ* process fully described elsewhere.[6] The pertinent deposition parameters: substrate temperature $T_s = 740$ °C; total pressure $(Ar + O_2)$ $P_T = 32$ Pa (240 mTorr) with $P_{O_2} = 13$ Pa(96 mTorr). With the dc power fixed at 120 W, the deposition rate was 0.7 nm/min, a rather low value due to the gun-substrate geometry. It took 7 h to deposit each film to a thickness of 300 nm. The films were deposited onto the {100} surfaces of MgO and $SrTiO_3$ single-crystal substrates. The substrate preparation is known to play a crucial role in the film morphology on MgO.[7] After solvent cleaning, the MgO crystals were annealed in an oxygen flow at 1100 °C for 12 h. The films on MgO and $SrTiO_3$ had a zero resistance T_c of 89.0 and 89.6 K, respectively, and a J_c of approximately 1×10^6 on MgO and 4×10^6 A/cm^2 on $SrTiO_3$ at 76 K and zero field.

The laser ablated films were prepared using a frequency tripled Nd-YAG laser operating at 355 nm with a repetition rate of 10 Hz. The films were grown at 775 °C in 27 Pa (200 mTorr) of oxygen at approximately 75 nm/min to a thickness of 100–200 nm. After deposition, the samples were cooled at 20 °C/min, while the chamber was backfilled with oxygen, held for 5 min at 470 °C in 80 kPa (600 Torr) of oxygen, and then slowly cooled to room temperature. This procedure routinely produces films with T_c between 90 and 91 K.

The growth mechanisms of YBCO films depend on the deposition technique and substrate material. Figure 1 shows screw dislocation growth on the surface of a sputtered film on MgO. Many screw dislocation spirals appear to merge into each other. Figure 2 shows that the topography of the sputtered YBCO on $SrTiO_3$ is quite different. The ledge-like structure shown was observed across the

 0003-6951/91/483039-03$02.00 © 1991 American Institute of Physics

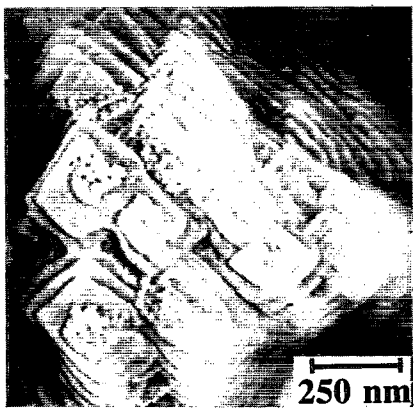

FIG. 1. Top-view STM image of a sputtered YBCO thin film on a {100} MgO substrate. The sample was scanned at room temperature in air.

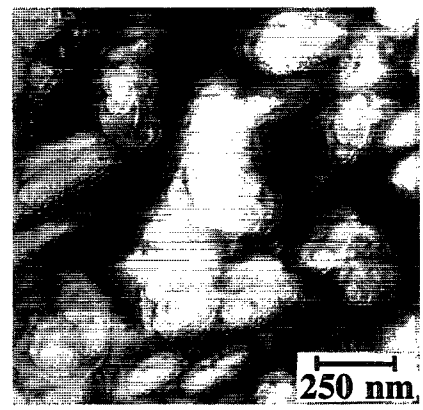

FIG. 3. Top-view STM image of a laser ablated YBCO thin film on a {100} $LaAlO_3$ substrate. The sample was scanned at room temperature in air.

entire surface of the film. Since the "top" of the growth structures was never found it is not possible to determine the growth mechanism. However, the resulting morphology is distinct from the images of Hawley *et al.*[2] and Gerber *et al.*[3] of sputtered YBCO on $SrTiO_3$, which show screw dislocation morphologies. An STM image of the surface of a laser ablated YBCO film on $LaAlO_3$ is shown in Fig. 3. Here growth appears to occur by ledge growth in concentric rings < 1 μm in size.

At first glance we might assume that the features in the STM images delineate grain boundaries. However, the films are relatively flat with surface roughness of < 10 nm. The films are about 200 nm thick, so that what appear to be large stacks of layers are in reality small features. These features are barely visible using high-resolution scanning electron microscopy (SEM). It is tempting to equate the spirals seen using STM with grains and their intersections with grain boundaries. We have found, however, that for films sputter deposited onto MgO and imaged by STM, screw-dislocation spacing is less than the grain size determined on similar samples using transmission electron microscopy (TEM) or scanning electron microscopy (SEM) of etched samples. The TEM and SEM show grain sizes that range from 0.5 to 10 μm in diameter. We conclude that several growth spirals exist on the surface of an average grain. It is also interesting that the grain (a and b axes) orientation, as observed by STM, is predominantly aligned with the MgO ⟨100⟩ direction except for a small percentage aligned with the MgO ⟨110⟩ direction. This is also observed by TEM and SEM.

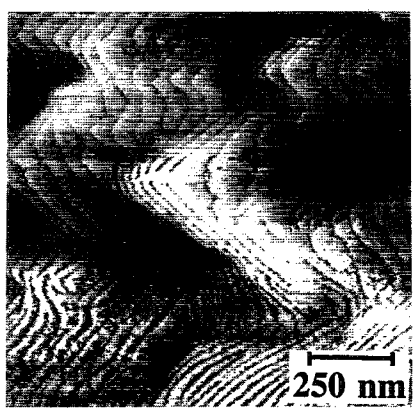

FIG. 2. Top-view STM image of a sputtered YBCO thin film on a {100} $SrTiO_3$ substrate. The sample was scanned at room temperature in air.

At room temperature, the height variations associated with the growth steps as imaged by the STM are anomalously large compared to the theoretical unit cell in the c-axis direction. We believe that variations in the surface barrier, density of states, or similar electronic effects cause these anomalies and that they do not represent the true topography of the samples. Hawley *et al.*[2] presented similar STM data. They have shown by performing atomic force microscopy (AFM), which should be unaffected by electronic effects, that the true step height is about 1.2 nm, as expected.

The STM step height is temperature dependent. As the temperature decreases from 300 K the height variation decreases, approaching the expected step-like profile with edge height equal to the unit cell value. The STM step height at 76 K is between 1 and 2 nm. Figure 4 is a STM image of a YBCO film sputtered onto MgO taken at 100 K. Figure 5 shows the surface profiles of a sputtered YBCO film on MgO taken at various temperatures ranging from 300 to 76 K. Notice the change from a sawtooth pattern to steps separated by flat regions. The STM step heights are plotted as a function of temperature in Fig. 6.

The origin of this striking temperature effect is uncertain. The STM images are maps of constant tunneling conductance plotted as height variations. The tunneling conductance reflects a density of unoccupied states on the film surface as well as tip effects. The step-height temperature may arise from the anisotropic properties of YBCO. Resistance measurements on YBCO single crystals show a semiconducting behavior perpendicular to the CuO planes (parallel to the c axis) and a metallic temperature dependence within the CuO planes.[8] Both of these will give rise to temperature-dependent tunneling of electrons into states parallel to the c axis. At a step edge there could be a

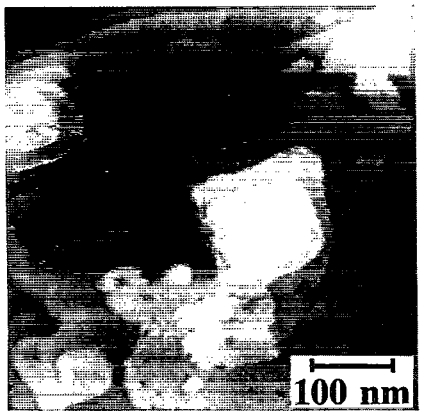

FIG. 4. Top-view STM image of a sputtered YBCO thin film on a {100} MgO substrate. The sample was scanned at 100 K in nitrogen gas.

difference in coupling between tip states and either the *c* axis or the *a-b* plane states causing temperature-dependent tunneling conductance. However, this mechanism would imply spatial variations at low temperatures while the data indicate that at low temperatures the tunneling conductance is uniform. Alternatively, the temperature-dependent step height may be associated with an oxygen depleted or chemically reacted surface layer. Both possibilities could lead to semiconducting phases whose composition and electronic properties would vary near step edges.

In summary, the STM can be used to image differences in the morphology of as-grown, *in situ* YBCO films deposited on various substrates by sputtering or laser ablation. The newly developed long scanning range capabilities combined with the superior vertical sensitivity make the STM unique for this type of application. The images are useful

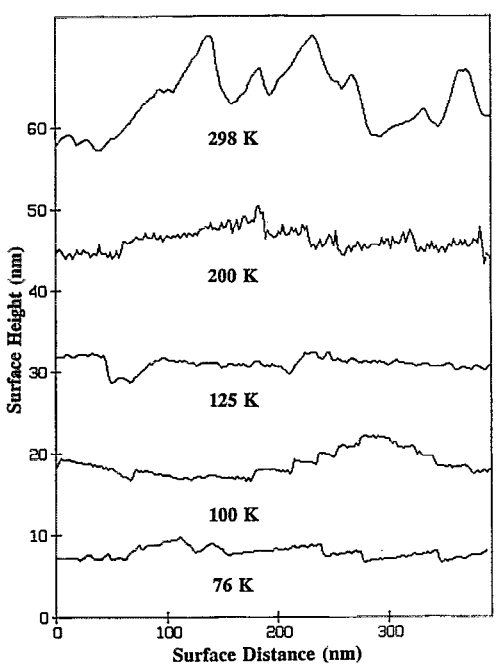

FIG. 5. Typical STM height profiles as a function of temperature for the sputtered YBCO thin film on MgO shown in Fig. 1.

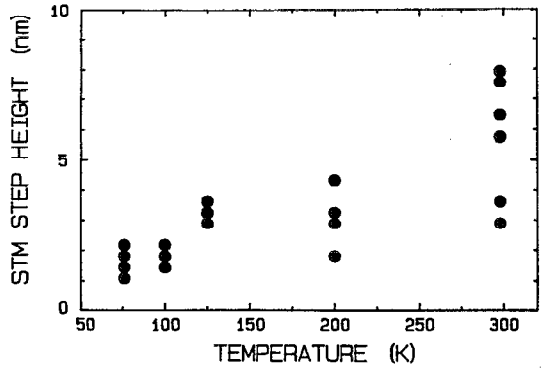

FIG. 6. STM step height vs temperature for the sputtered YBCO thin film on MgO shown in Figs. 1 and 4.

for determining the film growth mechanisms. Screw dislocations and surface roughness as seen in STM images may contribute to flux pinning. We have not seen any correlation of the critical current densities with the structures observed by STM, although detailed studies have yet to be done. We have observed a higher density of screw dislocations, but lower critical current densities, in YBCO films on MgO than in films on $SrTiO_3$. We have taken STM images of sputtered YBCO films at various temperatures. At room temperature, the images show anomalously large step heights, compared to the expected unit cell height of 1.2 nm. However, the observed step height is temperature dependent and decreases nearly to the expected value at 76 K. The tunneling characteristics that affect the STM image are important for understanding the electrical properties of the surfaces of YBCO films. Such information is needed for development of Josephson tunneling barriers and general electrical contact structures that would be useful for integrated circuit applications.

We gratefully acknowledge the support of R. Folsom, who helped construct the low-temperature STM apparatus, and M. Hawley for helpful discussions. J.M. was supported by the Department of Energy, Basic Energy Sciences under Contract No. DE-AI05-90ER14044. B.J. was supported by the Swiss National Science Foundation.

[1] M. D. Kirk, C. B. Eom, B. Oh, S. R. Spielman, M. R. Beasely, A. Kapitulnik, T. Geballe, and C. F. Quate, Appl. Phys. Lett. **52**, 2071 (1988); L. E. C. Van de Leemput, P. J. M. Van Bentum, L. W. M. Schreurs, and H. Van Kempen, Physica C **152**, 99 (1988); H. Heinzelmann, D. Anselmetti, R. Wiesendanger, H. J. Guentherodt, E. Kladis, and A. Wisard, Appl. Phys. Lett. **53**, 2447 (1988); H. J. Scheel and P. Neidermann, J. Cryst. Growth **94**, 281 (1989).
[2] M. Hawley, I. D. Raistrick, J. G. Berry, and R. J. Houlton, Science **251**, 1587 (1991).
[3] C. Gerber, D. Anselmetti, J. G. Bednorz, J. Mannhart, and D. G. Schlom, Nature **350**, 279 (1991).
[4] J. Moreland and P. Rice, IEEE Trans. Magn. **27**, 1198 (1991).
[5] J. Moreland, Y. Li, R. Folsom, and T. E. Capobianco, Rev. Sci. Instrum. **59**, 2535 (1988).
[6] S. E. Russek, B. Jeanneret, D. A. Rudman, and J. W. Ekin, IEEE Trans. Magn. **27**, 931 (1991).
[7] B. H. Moeckly, S. E. Russek, D. K. Lathrop, R. A. Buhrman, J. Li, and J. W. Mayer, Appl. Phys. Lett. **57**, 1687 (1990).
[8] S. J. Hagen, T. W. Jing, Z. Z. Wang, J. Horvath, and N. P. Ong, Phys. Rev. B **37**, 7928 (1988).